Exercises for the GGI 2025

Pedro de la Torre and Mattia Di Mauro

April 4, 2025

1 Exercise on DM production of cosmic-ray antimatter

1.1 Estimate the annihilation rate needed to explain the positron flux measured at 100 GeV

Measurements of the positron flux at high energies by PAMELA, and then, AMS-02, revealed that there must be a powerful source of positrons, different than cosmic-ray (CR) interactions with the gas in the interstellar medium (ISM), that dominates the spectrum above several tens of GeV (See Fig. 1).
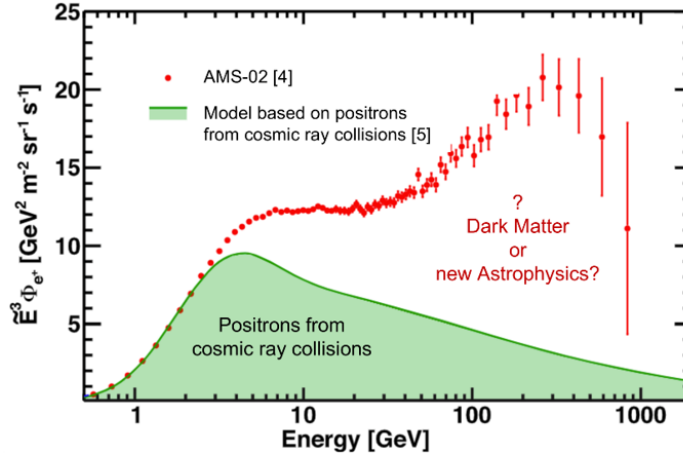
Figure 1: Positron flux measured by AMS-02 compared to the expectation of the secondary positron flux. Credit: AMS-02 collaboration.

Given that WIMPs could produce a significant amount of positrons when decaying/annihilating, one of the ideas that appeared to explain this "positron excess" was dark matter (DM). In this case, one can use a simplified version of the leaky-box approximation to estimate the local flux of positrons produced by DM at a given energy, E_{e^+}:

$$Q_\chi(E_{e^+}, r_\odot) - \frac{n_{e^+}}{\tau_{leak}}(E_{e^+}, r_\odot) = \frac{dn_{e^+}}{dt}(E_{e^+}, r_\odot), \tag{1}$$

for which we can find the steady state solution easily. Consider $\rho_\chi(r_\odot) \approx 0.4$ GeV/cm^3, $m_\chi \approx 1$ TeV and annihilation to the τ channel ($\chi + \chi \longrightarrow \tau^+ \tau^-$), which yields approximately $\frac{dN_{e^+}}{dE_{e^+}}(E_{e^+} = 100\,\text{GeV}) \approx 3.7 \cdot 10^{-3}$ GeV^{-1}.

Hint: The dominant time-scale for positrons of energies above tens of GeV is energy losses, mainly due to inverse-Compton and Synchrotron losses. For a simple estimation of the local loss time, use the expression:

$$\tau_{loss} \approx E_e / (\frac{dE}{dt}) = \frac{4}{3}\sigma_t \gamma_e^2 c(U_B + U_{CMB}) \approx 30.7 \left(\frac{E_e}{\text{GeV}}\right)^{-1} \left(\frac{U_B + U_{CMB}}{\text{eV/cm}^3}\right)^{-1} \quad \text{Myr,}$$

where σ_t is the Thomson cross sections, c is the speed of light, γ_e is the Lorentz factor of the electrons, $U_{CMB} \sim 0.26$ eV/cm^3 is the CMB energy density and $U_B = \frac{B^2}{4\pi}$ eV/cm^3 is the magnetic field energy density (where for local values one can use B$\sim 3 - 5 \, \mu$G).

Answer:
Eq. 1, assuming steady state $(\frac{dn_{e+}}{dt}(E_{e+}, r_\odot) = 0)$, becomes

$$Q_\chi(E_{e+}, r_\odot) \cdot \tau_{leak}(E_{e+}, r_\odot) = n_{e+}(E_{e+}, r_\odot), \tag{2}$$

where n_{e+} is the positron density per unit of energy, τ_{leak} is the dominant (effective) time-scale for positrons of energy E_{e+} to leak out and Q_χ is the source term of DM annihilation to produce the positrons, which is defined as

$$Q_\chi(E_{e+}, r_\odot) = \frac{\langle \sigma v \rangle}{2} \frac{\rho_\chi^2(r_\odot)}{m_\chi^2} \frac{dN_{e+}}{dE_{e+}}(E_{e+}), \tag{3}$$

assuming DM as a Majorana particle. Here, $\langle \sigma v \rangle$ is the annihilation rate to be estimated, $\rho_\chi(r_\odot) \approx 0.4$ GeV/cm^3 is the local DM density, the DM mass can be assumed to be the one providing the best-fit to the positron excess, $m_\chi \approx 1$ TeV and $\frac{dN_{e+}}{dE_{e+}}(E_{e+})$ is the injection spectrum of positrons produced per annihilation. For the latter, we can assume the τ channel $(\chi + \chi \longrightarrow \tau^+ \tau^-)$, which, at $E_{e+} = 100$ GeV, yields approximately $\frac{dN_{e+}}{dE_{e+}}(E_{e+}) \approx 3.7 \cdot 10^{-3}$ GeV^{-1} for a 1 TeV DM particle. To convert the density of positrons per unit of energy into flux, one can simply use: $\frac{d\phi_{e+}}{dE} = c \cdot n_{e+}/(4\pi)$, where c is the speed of light. Note that Eq. 2 is what you find neglecting all terms in the full diffusion equation but the injection term and the energy loss term.

We have to solve for $\langle \sigma v \rangle$ using Eq. 2, knowing that the measured local flux of positrons is $\frac{d\phi_{e+}^{AMS-02}}{dE} \approx 2.5 \cdot 10^{-10}$ cm^{-2} s^{-1} sr^{-1} GeV^{-1} at 100 GeV, and where $\tau_{loss} \sim 1$ Myr. Therefore, we simply need the solve the following formula:

$$\langle \sigma v \rangle = \frac{2m_\chi^2}{\rho_\chi^2(r_\odot)} \frac{1}{\frac{dN_{e+}}{dE_{e+}}} \frac{1}{\tau_{loss}} \frac{d\phi_{e+}^{AMS-02}}{dE} \frac{4\pi}{c} \sim 10^{-23} \text{cm}^3/\text{s}, \tag{4}$$

to reproduce the AMS-02 flux observed at $E_{e+} = 100$ GeV.

Conclusion: This value is similar, within a factor of 2, to what has been typically found. As you may notice, it is quite above the thermal relic cross sections, but it is also excluded by other indirect DM searches, using, e.g. radio or from γ-ray observations (See, for instance, Refs. [A$^+$11, B$^+$09]).

The dominant source of high-energy positrons is expected to be pulsars. There are several theoretical and observational arguments that support the idea that pulsars and their nebulae are positrons factories that can efficiently inject accelerate electrons/positrons up to such energies, as it is discussed in the main lectures..

1.2 Estimate the flux of antiprotons produced from DM at 10 GeV and compare with the expected flux produced from cosmic-ray interactions

After AMS-02 published their observations of the local antiproton spectrum, different groups pointed to a possible anomaly, an excess of antiprotons over the expected background at around 10 GeV. The DM signal required to fit it was roughly compatible with the thermal relic cross sections and a DM mass in the range of 40-90 GeV (See Fig. 2). Calculate the approximate flux of antiprotons that can be produced by DM annihilation into the $b\bar{b}$ channel and compare to the expected secondary antiproton flux.
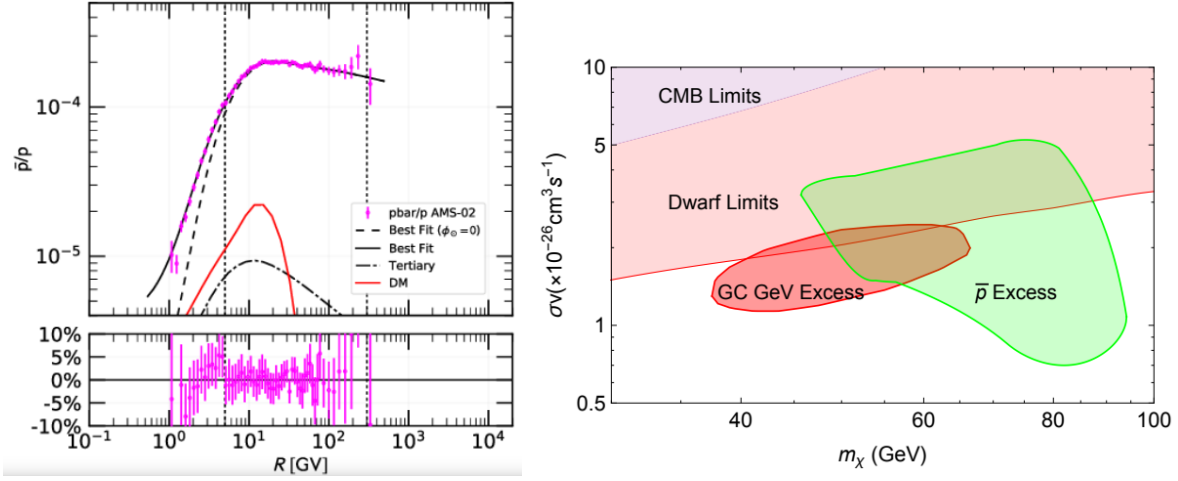
Figure 2: Left panel: Comparison of the AMS-02 $\bar{p}$/p ratio with the best-fit antiproton flux from DM and CR interactions [CKK17]. Right panel: Contour plot indicating the parameter space (annihilation rate vs DM mass) able to reproduce the $\bar{p}$ excess and the Galactic Centre excess [CLH19].

1.2.1 Compute DM flux for thermal annihilation cross sections

Hint: The dominant time scale in this case is the diffusion time scale (effective time that CRs remain confined in the Galaxy), $\tau_{diff}(E) = \frac{H^2}{2D(E)}$, where $H \approx 4$ kpc is the so-called halo height and $D \propto E^\delta$ is the effective diffusion coefficient ($D \approx 2.5 \cdot 10^{28}$ cm^2/s at 10 GeV). Take a value of $\frac{dN_{\bar{p}}}{dE_{\bar{p}}}(E_{\bar{p}} = 10\text{GeV}) \approx 2.3 \cdot 10^{-2}$ GeV^{-1} (corresponding to a 70 GeV DM particle annihilating in the $b\bar{b}$ channel).

Answer

Using Eq. 3 for this case, we get a value of $Q_\chi^{\bar{p}}(E_{\bar{p}} = 10\text{GeV}) \sim 10^{-32}$ cm^{-3} s^{-1} GeV^{-1} (with $\langle \sigma v \rangle = 2.3 \cdot 10^{-26}$ cm^3/s). Then, from Eq. 2 with $\tau_{leak} = \tau_{diff} \sim 100$ Myr [EMBA20], we get that

$$\frac{d\phi^{\bar{p}}}{dE}(E_{\bar{p}} = 10\text{GeV}) = Q_\chi^{\bar{p}}(E_{\bar{p}} = 10\text{GeV}) \times \tau_{diff} \times \frac{c}{4\pi} \sim 7 \cdot 10^{-8} \ \text{cm}^{-2}\,\text{s}^{-1}\,\text{sr}^{-1}\,\text{GeV}^{-1}.$$

This estimation is of the order of magnitude of the total antiproton flux observed at Earth, which is much larger than the correct value you get with the full calculation. As can be seen from recent analyses [CCD$^+$22, DlTLWL24a] the best-fit cross sections of the excess are a bit lower, quite close to $\langle \sigma v \rangle = 10^{-26}$ cm^3/s.

Caveats: The simple version of the leaky-box approximation used previously is not reliable here, because the local antiproton flux at 10 GeV has a larger contribution from antiprotons produced away from our local neighborhood (i.e. the effective DM density changes from the assumed local DM density due to propagation). In addition, other effects may become more relevant at this energy range: solar modulation, reacceleration or convection.

Conclusion: We saw that the approximations made in the previous case are not applicable to the estimation of the flux of antiprotons. However, the source term, that provides the production rate at injection, can be used to compare the DM signal with that expected from the background (CR collisions in the gas).

1.2.2 Compare with CR production

The source term for the production of antiproton from CR interactions with the ISM gas is given by

$$Q_{CR+ISM\to\bar{p}}(E_{\bar{p}}) = \sum_{ISM}\sum_{CR} 4\pi\, n_{ISM} \int_0^\infty dE\, \frac{d\sigma_{CR+ISM\to\bar{p}}}{dE_{\bar{p}}}(E,E_{\bar{p}})\, \frac{d\phi_{CR}}{dE}(E,r_\odot), \qquad (5)$$

where n_{ISM} stands for the density of gas of each element (the ISM is mainly composed by H and He with traces of heavier elements, with total density of approximately 1 cm^{-3}), $\frac{d\sigma_{CR+ISM\to\bar{p}}}{dE_{\bar{p}}}(E,E_{\bar{p}})$ is the differential cross section of a primary CR nucleus interacting with a gas element to produce antiprotons with energy $E_{\bar{p}}$, and $\frac{d\phi_{CR}}{dE}$ is the differential local flux of that primary CR. The integral is performed over the energy of the primary CR and the sums must be done for all primary CR species and gas elements in the ISM.

However, since the most abundant gas element in the ISM is H and the primary CRs are dominated by CR protons one can compute the source term (Eq. 5) considering only p-p collisions (by CR protons with H gas in the ISM) and still get an estimation that is acceptable (accurate within tens of percent). Furthermore, we will do another simplification to make this estimation quicker: since the source term strongly peaks at around $E_p = 70$ GeV, we will only consider the proton flux and differential cross section at $E_p = 70$ GeV and $E_{\bar{p}} = 10$ GeV to calculate $Q_{pp\to\bar{p}}$.

Hint: There are different cross sections parametrizations recently developed for antiproton production in CR interactions. You can quickly find the differential cross sections for this interaction in `https://github.com/cosmicrays/DRAGON2-Beta_version/blob/master/data/Winkler-ap_pp.dat`. The local proton flux can be found in any AMS-02 publication.

Answer

We have to solve for

$$Q_{CR}^{\bar{p}}(E_{\bar{p}} = 10 \text{ GeV}) \sim 4\pi n_H \frac{d\sigma_{pp\to\bar{p}}}{dE_{\bar{p}}}(E = 70 \text{ GeV}, E_{\bar{p}} = 10 \text{ GeV})\, \phi_p(E = 70 \text{ GeV}, r_\odot). \qquad (6)$$

Using Eq. 6, and adopting a differential cross section $\frac{d\sigma_{pp\to\bar{p}}}{dE_{\bar{p}}} \sim 5\cdot 10^{-2}$ mb/GeV for antiprotons produced at $E_{\bar{p}} = 10$ GeV and a CR proton interacting with energy $E_p = 70$ GeV and a local proton flux of $\phi_p \sim 8\cdot 10^{-4}$ cm^{-2} s^{-1} sr^{-1} (See supp. Material of Ref. [A$^+$15]), one gets a value around $Q_{CR}^{\bar{p}}(E_{\bar{p}} = 10 \text{ GeV}) \sim 4.5\cdot 10^{-31}$ cm^{-3} s^{-1} GeV^{-1}.

Now, comparing the DM source term with this, we obtain:

$$\frac{Q_{DM}^{\bar{p}}}{Q_{CR}^{\bar{p}}} \sim \frac{n_{DM}^{\bar{p}}}{n_{CR}^{\bar{p}}} \sim 0.02\,,$$

which is not too far from the value that we find with detailed calculations. We show the antiproton source term computed in the left panel of Fig. 3. Notice that this is a small fraction of the total flux, making it more difficult to confirm given that the systematic uncertainties in these calculations are greater than 10%, especially from cross sections or correlated errors in the AMS-02 measurements.

1.3 Estimation of Antinuclei production

Antinuclei are considered one of the most promising smoking guns for the study of DM, since the production of such particles from CR interactions is very suppressed (see right panel of Fig. 4). In the last years, the AMS-02 collaboration has claimed the detection of a few antinuclei events (See Fig. 4), which challenge our current models of production of antihelium in the Galaxy. We can do a similar calculation to that we did before to estimate the flux of an antinucleus produced from DM annihilation/decay and from CR interactions with gas.
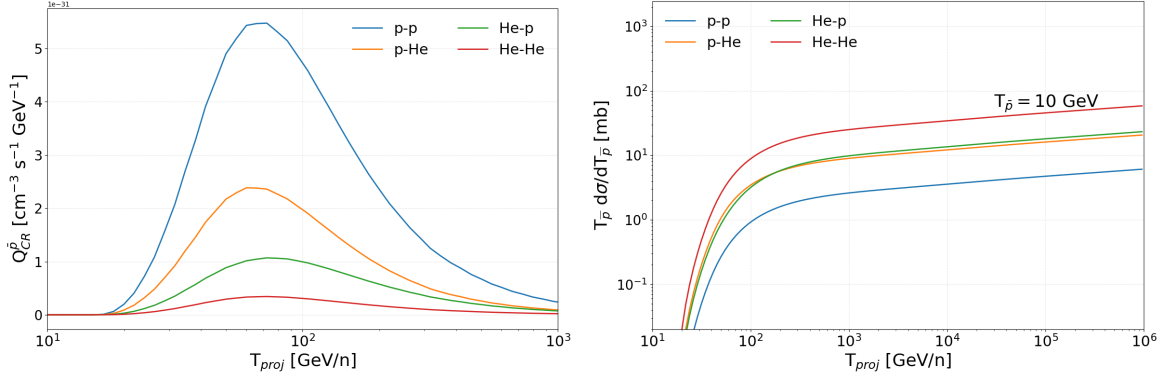
Figure 3: Left panel: Source terms for the main interactions of CRs with ISM gas to produce $\bar{p}$ at an energy of 10 GeV, as a function of the projectile energy. Right panel: Cross sections for the production of $\bar{p}$ at an energy of 10 GeV for each of the main interaction channels.
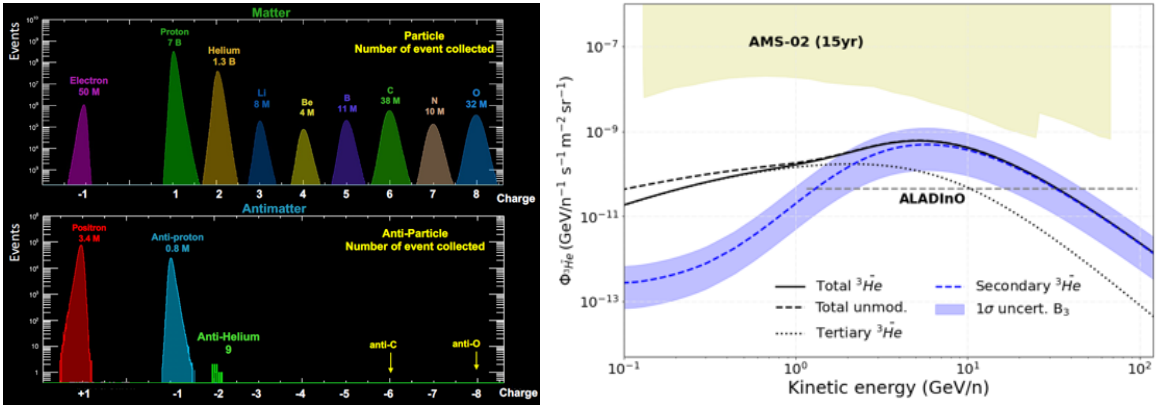
Figure 4: Left panel: Representation of the events recorded by AMS-02 as a function of their charge. Credit: Paolo Zuccon (MIAPP 2021). Right panel: Flux of antihelium-3 expected from CR interactions compared to the sentitivity of AMS-02 [DLTLWL24b].

In the spherical coalescence approximation, the injection spectrum of an antinucleus $\bar{A}$ can be approximated from the injection spectrum of the antiprotons and antineutrons produced

$$\frac{dN}{dE_{\bar{A}}} \propto \left(\frac{dN}{dE_{\bar{p}}}\right)^Z \left(\frac{dN}{dE_{\bar{n}}}\right)^{(A-Z)} , \tag{7}$$

where A and Z are the atomic and mass number of the antinucleus.

This expression can be further simplified if considering that the production of neutrons and protons is roughly the same (which is not strictly true, see, e.g., Ref. [Win17]). Adding also the constant factors to the previous equation and using this simplification, one gets:

$$\frac{dN}{dE_{\bar{A}}} (E_{\bar{A}} = E_{\bar{p}}/A) \sim B_{\bar{A}} \frac{A}{(4\pi)^{A-1}} \frac{1}{\left(E_{\bar{p}}^2 + 2m_{\bar{p}}E_{\bar{p}}\right)^{(A-1)/2}} \left(\frac{dN}{dE_{\bar{p}}}\right)^A , \tag{8}$$

where A is the atomic number of the antinucleus $\bar{A}$ that we are evaluating and $B_{\bar{A}}$ is the coalescence factor, defined as:

$$B_{\bar{A}} = \left(\frac{1}{8}\frac{4}{3}\pi p_c^3\right)^{A-1} \frac{m_{\bar{A}}}{m_{\bar{p}}^Z m_{\bar{n}}^{(A-Z)}} , \tag{9}$$

being p_c the coalescence momentum, which accounts for the distance in momentum space that A antinucleons must be to form the antinucleus $\bar{A}$, and it is commonly evaluated from accelerator data. Eq. 8 must be evaluated at an antiproton energy $E_{\bar{p}} = A \cdot E_{\bar{A}}$.

This expression neglects correlations, which is especially important for DM production of antinuclei, and would require to use event-by-event generators like Pythia or Herwig. However, for the DM mass and channel that we use, this gives us a conservative underestimation (See Fig of Ref. [DK12]). In turn, for the case of CR production, correlations become less important.

1.3.1 Compare the DM source term with that from CRs for the production of antihelium-3 at 1 GeV, considering the same DM particle as in the previous question

Hint: Take $p_c \sim 225$ MeV (See Fig. 1 of Ref. [DLTLWL24b]) and compare with the source term for secondary production shown in Fig. 1 of Ref. [KDF18], where $Q_{pp}^{3\overline{He}}(E_{3\overline{He}} \sim 1 \text{ GeV}) \sim 5{\cdot}10^{-46}$ cm^{-3} s^{-1} GeV^{-1}.

_____

Answer:
First, we can compute the coalescence factor, which is

$$B_{\bar{3}} = \left(\frac{1}{8}\frac{4}{3}\pi p_c^3\right)^2 \frac{m_{3\overline{He}}}{m_{\bar{p}}^2 m_{\bar{n}}} \sim 1.2 \cdot 10^{-4} \text{ GeV}^4, \tag{10}$$

The DM injection spectrum for the production of $^3\overline{He}$ is:

$$\frac{dN_{3\overline{He}}}{dE_{3\overline{He}}}(E_{3\overline{He}} = 1 \text{ GeV}) \sim B_3 \frac{3}{(4\pi)^2}\frac{1}{\left(E_{\bar{p}}^2 + 2m_{\bar{p}}E_{\bar{p}}\right)}\left(\frac{dN_{\bar{p}}}{dE_{\bar{p}}}\right)^3_{E_p = 3 \text{ GeV}}. \tag{11}$$

Therefore, the source term for DM becomes:

$$Q_{DM}^{3\overline{He}}(E_{3\overline{He}} = 1 \text{ GeV}) \sim \frac{\langle\sigma v\rangle}{2}\frac{\rho_\chi^2(r_\odot)}{m_\chi^2}\frac{3B_3}{(4\pi)^2}\frac{1}{\left(E_{\bar{p}}^2 + 2m_{\bar{p}}E_{\bar{p}}\right)}\left(\frac{dN_{\bar{p}}}{dE_{\bar{p}}}\right)^3_{E_p = 3 \text{ GeV}} \tag{12}$$

$$Q_{DM}^{3\overline{He}}(E_{3\overline{He}} = 1 \text{ GeV}) \sim 6 \cdot 10^{-41} \text{ cm}^{-3}\text{ s}^{-1}\text{ GeV}^{-1},$$

which is pretty similar to the value obtained with a more detailed (but still analytical) calculation [KDF18].

Comparing both source terms, we see that we expect at least 10^4 times more production of $^3\overline{He}$ from DM annihilation than from CR production (as shown in Fig. 1 of Ref. [KDF18]), making antinuclei a powerful smoking gun for DM searches.

Note: Going to lower energies the difference between the expected DM and CR contribution becomes larger. Do you have an explanation for this? Compute the threshold energy to produce antideuterons and antihelium from p-p interactions.

2 Secondary emission from light and heavy dark matter: Inverse-Compton and Synchrotron

A variety of works have used secondary emissions to set constraints on light or heavy DM candidates, below and above the WIMP mass range. For example, Ref. [LN24] studied the inverse-Compton (IC) emission from the interaction of the electrons, produced in the annihilation/decay of DM, with the radiation fields of the Galaxy. In this way, they were able to set constraints from Fermi-LAT measurements for DM candidates whose prompt emission lies at energies much higher than those accessible for Fermi. Similarly, Refs. [CFK+23] and [DlTLKB24] used a similar procedure, that allowed to set constraints on sub-GeV DM and asteroid-mass primordial black holes, respectively, with X-ray observations.

Similarly, the synchrotron emission can be used to set constraints on a broad set of DM candidates. Radio synchrotron emission has been used to constrain WIMPs, but it can be used to constrain heavier candidates, with emissions falling in the X-ray and gamma-ray energy ranges.

In this exercise, we will estimate and discuss how these secondary emissions can allow us to obtain constraints for DM candidates beyond WIMPs.

2.1 Estimate the peak energy of inverse-Compton emission from a DM particle decaying into electrons. Assume a mass of ~ 100 MeV and ~ 1 GeV for different radiation fields.

Essentially, IC scattering consists of high-energy electrons up-scattering ambient photons with energy E_{RF} (where RF stands for radiation field) to an energy $\gamma^2 E_{RF}$, where γ is the Lorentz factor of the electrons injected. For our case, this means that for the decay into electrons of a DM particle with mass m_χ in a radiation field with photons at a given energy will be up-scattered to an energy:

$$E = \gamma^2 E_{RF} \rightarrow E \sim \left(\frac{m_\chi}{2m_e}\right)^2 E_{RF}\,, \tag{13}$$

as long as the injected energy of the photons is below the Klein-Nishina regime.

Since radiation fields aren't monochromatic, one can estimate the energy at the peak emission, using

$$E_{peak} \sim \left(\frac{m_\chi}{2m_e}\right)^2 E_{RF}^{peak} \tag{14}$$

Given that the CMB photons are detected with temperature ~ 2.73 K, one gets that the peak energy of this photon field is $\sim 6 \cdot 10^{-4}$ eV. Consider also infrared field, peaking around $9 \cdot 10^{-3}$ eV and starlight peaking around 1 eV (see Ref. [LV18]).

At which energies do you expect to have IC emission from the interaction of DM electrons with these radiation fields? Which measurements could we use?
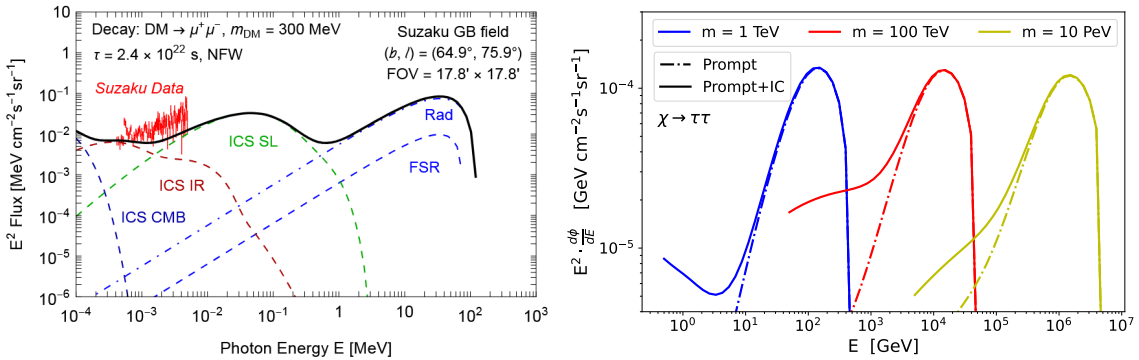
Figure 5: Left panel: IC emission for the decay of a 300 MeV DM particle into muons [CFK+23]. Right panel: Prompt and IC gamma–ray emission of heavy DM decaying in the τ channel.

———————

Answer

For a 100 MeV particle, the peak IC emission will lie at around 6 eV, 0.09 keV and ~ 10 keV for the CMB, IR and starlight radiation fields, respectively. For a 1 GeV particle, these would be around 0.6 keV, 8.6 keV and ~ 0.1 MeV.

Therefore, this constitutes a broad band emission that can be probed with multimessenger observations, covering from optical or UV observations, to X–rays and soft gamma–rays.

2.2 Estimate the peak frequency of synchrotron emission heavy DM

Synchrotron emission from the WIMPs decaying into electrons have been usually searched for in the radio band. Using Eq. 15, we can compute the critical frequency of the emission from a heavy DM particle decaying to electrons and find the frequency range where this emission can be expected. Take a perpendicular (with respect to our line of sight) component of the magnetic field $B_\perp \sim 5\,\mu$G. Can this emission be observed at ground?

$$\nu_{crit}(\text{GHz}) = \frac{3e}{4\pi m_e} B_\perp \gamma^2 \sim 4.2 \left(\frac{B}{G}\right) \gamma^2 \text{ MHz}. \tag{15}$$

The critical frequency gives an estimation of the peak frequency generated by the synchrotron interaction of electrons with energy E and the perpendicular component of the magnetic field which they interact with.

Calculate the expected frequency range for synchrotron emission from a 10 EeV, 200 GeV and a 1 GeV DM particle.

———————

Answer

The critical frequency is ~ 20 MHz, ~ 200 GHz and $\sim 2 \cdot 10^{16}$ GHz (~ 41 GeV), for the decaying DM with masses 1 GeV, 200 GeV and 1 EeV (i.e. 10^9 GeV), respectively.

In the ultra-heavy case, Ref. [MP24] recently showed that the peak energy of this emission for ultra-heavy DM can lie in the Fermi-LAT range and derived constraints on such ultra-heavy DM.

3 The Galactic Centre Excess (GCE)

The GCE excess is one of the most debated astrophysical anomalies that have been related to DM. Many years after the first evidences, there is a warm debate in the community about its origin. We will quantitatively discuss the DM case and compare it to the pulsar case.

3.1 Determine the Annihilation Cross Section corresponding to the GCE flux

There are several indications that suggest that DM can be the origin of this excess. Here we will see that its observed intensity can be well compatible with a WIMP and discuss some other factors that make this hypothesis appealing.

To match the predicted DM gamma–ray flux with the observed flux, one can use the flux formula, Eq. 16. Suppose that the observed integrated flux (over a chosen energy range) is Φ_{obs}. Then

$$\Phi_{\text{obs}} = \frac{\langle \sigma v \rangle}{8\pi \, m_\chi^2} \, N_\gamma \, J \,, \tag{16}$$

where N_γ is the total number of photons produced per annihilation (integrated over the energy range where the excess is observed).

Assuming an NFW profile (i.e. with an inner slope of $\gamma = 1$) the J-factor within the inner $20°$, corresponding to $\Delta\Omega \sim 0.1$ sr (that contains well the GCE), typically falls in the range

$$J \sim 10^{22} - 10^{23} \, \text{GeV}^2 \, \text{cm}^{-5}$$

Let us take:

- $m_\chi \simeq 50$ GeV (see Table 4 of Ref. [CCW15]) so that $m_\chi^2 \simeq 2500$ GeV^2,

- Take as a representative value for the J-factor

$$J \simeq 7 \times 10^{22} \, \text{GeV}^2 \, \text{cm}^{-5} \,. \tag{17}$$

- a photon yield $N_\gamma \sim 20$ (appropriate for the $b\bar{b}$ channel in the 1–10 GeV range),

- an observed flux $\Phi_{\text{obs}} \sim 10^{-6}$ ph/cm^2/s.

Answer

Inverting Eq. 16, we obtain

$$\langle \sigma v \rangle = \frac{8\pi \, m_\chi^2 \, \Phi_{\text{obs}}}{N_\gamma \, J} \,. \tag{18}$$

Let us perform the arithmetic step by step:

1. The numerator:
$$8\pi \times 2500 \simeq 25.13 \times 2500 \simeq 6.28 \times 10^4 \,.$$

2. Multiplying by 10^{-6} gives 6.28×10^{-2}.

3. The denominator is $20 \times 7 \times 10^{22} = 1.4 \times 10^{24}$.

4. Thus,
$$\langle \sigma v \rangle \simeq \frac{6.28 \times 10^{-2}}{1.4 \times 10^{24}} \simeq \frac{8\pi \times 2500 \times 10^{-6}}{20 \times 7 \times 10^{22}} = 4.5 \times 10^{-26} \, \text{cm}^3/\text{s} \,.$$

This value is of the same order as the canonical "thermal relic" cross section ($\sim 3 \times 10^{-26}\,\mathrm{cm^3/s}$) and is similar to the values reported in studies such as Ref. [DM21, DMW21].

Final Comments: This derivation illustrates one way to go from assumed halo properties and the observed gamma–ray excess to an inferred value of the DM annihilation cross section. In a more detailed analysis one would incorporate the full energy spectrum (using codes such as PPPC4DMID), account for uncertainties in the inner halo profile, and perform precise numerical integrations over the ROI. Nonetheless, the numbers obtained here are broadly in line with those reported in the literature.

3.2 Pulsar interpretation of the GCE

One of the leading explanations for the GCE is that the excess originates from an unresolved population of millisecond pulsars (MSPs). We now explore a pulsar interpretation for the Fermi–LAT Galactic GCE.

Let's simplify again our calculation to get a simple estimate of the number of MSPs that are required to account for the GCE. Assume that the integration over the spatial volume (over the region where the pulsars are distributed) yields a total number of pulsars N_{tot}, and that their luminosities can be characterized by an average luminosity $\langle L \rangle$ that can be estimated from observations or theoretical arguments. Under these assumptions the total flux becomes

$$\Phi_{\mathrm{tot}} \approx \frac{N_{\mathrm{tot}}\,\langle L \rangle}{4\pi d_{\mathrm{eff}}^2}\,, \tag{19}$$

where d_{eff} is an effective distance to the pulsar population. Since we are considering pulsars in the Galactic bulge, we set

$$d_{\mathrm{eff}} \sim d_{\mathrm{GC}} \sim 8.5\,\mathrm{kpc}\,.$$

Estimate the total number of MSPs that can account for the flux observed by Fermi-LAT. Take an average gamma–ray luminosity per pulsar: $\langle L \rangle \sim 10^{34}\,\mathrm{erg/s}$, which is based on several studies of the GCE and of pulsar populations.

––––––––

Answer:
Let's reorder Eq. 19:

$$N_{\mathrm{tot}} \sim \frac{\Phi_{\mathrm{obs}}\,4\pi d_{\mathrm{eff}}^2}{\langle L \rangle}\,, \tag{20}$$

First, convert the distance to centimeters. With

$$1\,\mathrm{kpc} \approx 3.086 \times 10^{21}\,\mathrm{cm}\,,$$

we obtain

$$d_{\mathrm{eff}} \approx 8.5\,\mathrm{kpc} \approx 8.5 \times 3.086 \times 10^{21}\,\mathrm{cm} \approx 2.62 \times 10^{22}\,\mathrm{cm}\,.$$

Then,

$$4\pi\,d_{\mathrm{eff}}^2 \approx 4\pi\,(2.62 \times 10^{22}\,\mathrm{cm})^2 \approx 4\pi \times 6.86 \times 10^{44}\,\mathrm{cm^2}\,.$$

Evaluating the denominator,

$$4\pi \times 6.86 \times 10^{44}\,\mathrm{cm^2} \approx 8.62 \times 10^{45}\,\mathrm{cm^2}\,.$$

Then, let's convert the flux observed ($\phi_{obs} \sim 10^{-6}\,\mathrm{ph\,cm^{-2}s^{-1}}$ at 1 GeV) into units of ergs/cm^2/s:

$$E\,\phi_{obs} \sim 10^{-6}\,\mathrm{GeV\,cm^{-2}s^{-1}} \approx 1.6 \cdot 10^{-9}\,\mathrm{erg\,cm^{-2}s^{-1}}$$

Thus,

$$N_{\mathrm{tot}} \sim \frac{1.6 \cdot 10^{-9}\,\mathrm{erg\,cm^{-2}s^{-1}}\,\;8.62 \cdot 10^{45}\,\mathrm{cm^2}}{10^{34}\,\mathrm{erg/s}} \sim 1400\,, \tag{21}$$

Meaning that we expect around a thousand MSPs around the Galactic Centre to explain the GCE. This value is well within the ballpark of more detailed estimations that take into account the spectral emission of MSPs, their distribution and luminosity distribution function (dN/dL).

A more detailed treatment would involve performing the following integral, over the pulsar luminosity function and the spatial volume,

$$\Phi_{\text{tot}} = \int dV \int_{L_{\text{min}}}^{L_{\text{max}}} dL \, \frac{dN}{dL} \, \frac{L}{4\pi d^2} \,, \tag{22}$$

and would include the spectral shape of individual pulsars given by

$$\frac{dN}{dE} \propto E^{-\Gamma} \, \exp\left(-\frac{E}{E_{\text{cut}}}\right)$$

with $\Gamma \sim 1.5$ and $E_{\text{cut}} \sim 2\text{–}3\,\text{GeV}$. Such an analysis would allow one to compare the predicted energy spectrum to the observed spectrum of the GCE. However, the simple estimate above shows that it is plausible for a population of $\sim 10^3$ pulsars with average luminosity $\sim 10^{34}$ erg/s to yield a total gamma–ray flux of the correct order of magnitude.

3.2.1 Integrating the Luminosity Function

Let the differential number of pulsars per unit luminosity be given by

$$\frac{dN}{dL} = A \, L^{-\alpha} \,, \qquad L_{\text{min}} \leq L \leq L_{\text{max}} \,, \tag{23}$$

where $\alpha > 1$ is the slope, and A is a normalization constant determined by the total number of pulsars,

$$N_{\text{tot}} = \int_{L_{\text{min}}}^{L_{\text{max}}} \frac{dN}{dL} \, dL = A \int_{L_{\text{min}}}^{L_{\text{max}}} L^{-\alpha} \, dL = A \, \frac{L_{\text{max}}^{1-\alpha} - L_{\text{min}}^{1-\alpha}}{1 - \alpha} \,. \tag{24}$$

Thus, the normalization is

$$A = N_{\text{tot}} \, \frac{\alpha - 1}{L_{\text{min}}^{1-\alpha} - L_{\text{max}}^{1-\alpha}} \,. \tag{25}$$

For an individual pulsar with luminosity L, the bolometric gamma–ray flux at Earth (assuming an effective distance d_{eff}) is

$$\Phi(L, d_{\text{eff}}) = \frac{L}{4\pi d_{\text{eff}}^2} \,. \tag{26}$$

Then the total flux from the population is

$$\Phi_{\text{tot}} = \frac{1}{4\pi d_{\text{eff}}^2} \int_{L_{\text{min}}}^{L_{\text{max}}} L \, \frac{dN}{dL} \, dL = \frac{A}{4\pi d_{\text{eff}}^2} \int_{L_{\text{min}}}^{L_{\text{max}}} L^{1-\alpha} \, dL \,. \tag{27}$$

Performing the integral (for $\alpha \neq 2$)

$$\int_{L_{\text{min}}}^{L_{\text{max}}} L^{1-\alpha} \, dL = \frac{L_{\text{max}}^{2-\alpha} - L_{\text{min}}^{2-\alpha}}{2 - \alpha} \,, \tag{28}$$

we obtain

$$\Phi_{\text{tot}} = \frac{A}{4\pi d_{\text{eff}}^2} \, \frac{L_{\text{max}}^{2-\alpha} - L_{\text{min}}^{2-\alpha}}{2 - \alpha} \,. \tag{29}$$

Substituting for A from Eq. (24) we find

$$\Phi_{\text{tot}} = \frac{N_{\text{tot}}}{4\pi d_{\text{eff}}^2} \, \frac{\alpha - 1}{2 - \alpha} \, \frac{L_{\text{max}}^{2-\alpha} - L_{\text{min}}^{2-\alpha}}{L_{\text{min}}^{1-\alpha} - L_{\text{max}}^{1-\alpha}} \,. \tag{30}$$

Many studies find that a value of $\alpha \sim 1.5$ is reasonable. You can assume the luminosity to be in the range of $L_{\min} = 10^{33}$ erg/s to $L_{\max} = 10^{35}$ erg/s. Use these values, along with a total number of MSPs of 10^3 to estimate the total flux expected from this population of sources.

—————

Answer:

For $\alpha = 1.5$, we have

$$\alpha - 1 = 0.5\,, \quad 2 - \alpha = 0.5\,.$$

Then Eq. (30) becomes

$$\Phi_{\text{tot}} = \frac{N_{\text{tot}}}{4\pi d_{\text{eff}}^2} \frac{0.5}{0.5} \frac{L_{\max}^{0.5} - L_{\min}^{0.5}}{L_{\min}^{-0.5} - L_{\max}^{-0.5}}$$

$$= \frac{N_{\text{tot}}}{4\pi d_{\text{eff}}^2} \frac{\sqrt{L_{\max}} - \sqrt{L_{\min}}}{\frac{1}{\sqrt{L_{\min}}} - \frac{1}{\sqrt{L_{\max}}}}\,. \tag{31}$$

Noting that

$$\frac{\sqrt{L_{\max}} - \sqrt{L_{\min}}}{\frac{1}{\sqrt{L_{\min}}} - \frac{1}{\sqrt{L_{\max}}}} = \sqrt{L_{\min} L_{\max}}\,, \tag{32}$$

we obtain the simple result

$$\Phi_{\text{tot}} = \frac{N_{\text{tot}} \sqrt{L_{\min} L_{\max}}}{4\pi d_{\text{eff}}^2}\,. \tag{33}$$

For representative numbers:

- Total number of pulsars: $N_{\text{tot}} = 10^3$,

- Minimum luminosity: $L_{\min} = 10^{33}$ erg/s,

- Maximum luminosity: $L_{\max} = 10^{35}$ erg/s,

- Effective distance: $d_{\text{eff}} = 8.5$ kpc.

First, we compute

$$\sqrt{L_{\min} L_{\max}} = \sqrt{10^{33} \times 10^{35}} = \sqrt{10^{68}} = 10^{34} \text{ erg/s}\,.$$

Next, converting d_{eff} to cm:

$$1\,\text{kpc} \approx 3.086 \times 10^{21}\,\text{cm} \quad \Longrightarrow \quad d_{\text{eff}} \approx 8.5 \times 3.086 \times 10^{21}\,\text{cm} \approx 2.623 \times 10^{22}\,\text{cm}\,.$$

Then,

$$4\pi\, d_{\text{eff}}^2 \approx 4\pi \times (2.623 \times 10^{22})^2 \approx 4\pi \times 6.88 \times 10^{44} \approx 8.64 \times 10^{45}\,\text{cm}^2\,.$$

Thus, the total flux is

$$\Phi_{\text{tot}} = \frac{10^3 \times 10^{34}}{8.64 \times 10^{45}} \approx 1.16 \times 10^{-9}\,\text{erg/cm}^2/\text{s}\,.$$

3.2.2 Including the Spectral Shape

Individual pulsars are observed to have gamma–ray spectra of the form

$$\frac{dN}{dE} \propto E^{-\Gamma} \exp\left(-\frac{E}{E_{\text{cut}}}\right)\,, \tag{34}$$

with a typical spectral index $\Gamma \sim 1.5$ and an exponential cutoff energy $E_{\text{cut}} \sim 2\text{–}3$ GeV.

If we wish to express the differential flux (in, say, $\text{erg}/\text{cm}^2/\text{s}/\text{GeV}$) we can write

$$\frac{d\Phi}{dE} = \Phi_{\text{tot}} \frac{S(E)}{N_S} \,, \tag{35}$$

where

$$S(E) = E^{-\Gamma} \exp\left(-\frac{E}{E_{\text{cut}}}\right)$$

describes the spectral shape and N_S is the normalization factor ensuring that

$$\int_{E_{\text{min}}}^{E_{\text{max}}} \frac{S(E)}{N_S} \, dE = 1 \,.$$

In many cases the normalization is written in terms of the incomplete Gamma function. For example, if we set $E_{\text{min}} = 0$ and $E_{\text{max}} \to \infty$, one obtains

$$N_S = \int_0^\infty E^{-\Gamma} \exp\left(-\frac{E}{E_{\text{cut}}}\right) dE = E_{\text{cut}}^{1-\Gamma} \, \Gamma(1 - \Gamma) \,,$$

with the understanding that for $\Gamma = 1.5$ the Gamma function is evaluated at $1 - 1.5 = -0.5$ (and one must be careful with the normalization). In a realistic analysis one would choose finite bounds (e.g. $E_{\text{min}} = 0.1$ GeV and $E_{\text{max}} = 100$ GeV).

Thus, the full differential flux, given by Eq. (35), becomes:

$$\frac{d\Phi}{dE} = \frac{N_{\text{tot}} \sqrt{L_{\text{min}} L_{\text{max}}}}{4\pi d_{\text{eff}}^2} \frac{E^{-\Gamma} \exp\left(-\frac{E}{E_{\text{cut}}}\right)}{N_S} \,. \tag{36}$$

3.2.3   Estimate the number of pulsars above the LAT sensitivity

Fermi–LAT detects a point source if its flux exceeds a threshold F_{th}. For the Galactic center region, we can adopt a value of

$$F_{\text{th}} \sim 3 \times 10^{-12} \text{ erg}/\text{cm}^2/\text{s} \,.$$

The flux from an individual pulsar of luminosity L is

$$\Phi(L) = \frac{L}{4\pi d_{\text{eff}}^2} \,. \tag{37}$$

A pulsar is detectable if $\Phi(L) \geq F_{\text{th}}$. Thus, the threshold luminosity L_{th} is determined by

$$L_{\text{th}} = 4\pi d_{\text{eff}}^2 \, F_{\text{th}} \,. \tag{38}$$

Then, the fraction of pulsars with luminosity $L \geq L_{\text{th}}$ is given by

$$f = \frac{\displaystyle\int_{L_{\text{th}}}^{L_{\text{max}}} L^{-\alpha} \, dL}{\displaystyle\int_{L_{\text{min}}}^{L_{\text{max}}} L^{-\alpha} \, dL} = \frac{L_{\text{th}}^{1-\alpha} - L_{\text{max}}^{1-\alpha}}{L_{\text{min}}^{1-\alpha} - L_{\text{max}}^{1-\alpha}} \,. \tag{39}$$

For $\alpha = 1.5$ we have $1 - \alpha = -0.5$, so that

$$f = \frac{L_{\text{th}}^{-0.5} - L_{\text{max}}^{-0.5}}{L_{\text{min}}^{-0.5} - L_{\text{max}}^{-0.5}} \,. \tag{40}$$

First, calculate the threshold luminosity. With that value, compute the fraction of pulsars with $L \geq L_{\text{th}}$ and the number of expected MSPs detected by Fermi-LAT around the Galactic Centre.

––––––––––

Answer:

We first convert the effective distance to centimeters. Using

$$1 \text{ kpc} \approx 3.086 \times 10^{21} \text{ cm} \,,$$

we have

$$d_{\text{eff}} \approx 8.5 \text{ kpc} \approx 8.5 \times 3.086 \times 10^{21} \text{ cm} \approx 2.62 \times 10^{22} \text{ cm} \,.$$

Then, calculating

$$4\pi d_{\text{eff}}^2 \approx 4\pi \left(2.62 \times 10^{22} \text{ cm}\right)^2 \,,$$

we find:

$$4\pi d_{\text{eff}}^2 \approx 4\pi \times \left(6.88 \times 10^{44} \text{ cm}^2\right) \approx 8.64 \times 10^{45} \text{ cm}^2 \,.$$

Thus, from Eq. (38) we obtain:

$$L_{\text{th}} \approx 8.64 \times 10^{45} \text{ cm}^2 \times 3 \times 10^{-12} \text{ erg/cm}^2/\text{s} \approx 2.59 \times 10^{34} \text{ erg/s} \,.$$

Now, we proceed to compute the fraction of detectable sources, using Eq.38.

- $\sqrt{L_{\text{min}}} = \sqrt{10^{33}} = 10^{16.5}$. Numerically,

$$10^{16.5} \approx 3.16 \times 10^{16} \text{ (in appropriate units)} \,.$$

- $\sqrt{L_{\text{max}}} = \sqrt{10^{35}} = 10^{17.5} \approx 3.16 \times 10^{17} \,.$

- $\sqrt{L_{\text{th}}} = \sqrt{2.59 \times 10^{34}} \approx 1.61 \times 10^{17} \,.$

Taking reciprocals, we have:

$$L_{\text{min}}^{-0.5} = \frac{1}{\sqrt{L_{\text{min}}}} \approx \frac{1}{3.16 \times 10^{16}} \approx 3.16 \times 10^{-17} \,,$$

$$L_{\text{th}}^{-0.5} = \frac{1}{\sqrt{L_{\text{th}}}} \approx \frac{1}{1.61 \times 10^{17}} \approx 6.21 \times 10^{-18} \,,$$

$$L_{\text{max}}^{-0.5} = \frac{1}{\sqrt{L_{\text{max}}}} \approx \frac{1}{3.16 \times 10^{17}} \approx 3.16 \times 10^{-18} \,.$$

Plug these values into Eq. (40):

$$f = \frac{6.21 \times 10^{-18} - 3.16 \times 10^{-18}}{3.16 \times 10^{-17} - 3.16 \times 10^{-18}} = \frac{3.05 \times 10^{-18}}{2.84 \times 10^{-17}} \approx 0.107 \,.$$

Thus, approximately 10.7% of the pulsars have luminosities above the detection threshold.

If the total number of pulsars is N_{tot}, then the number of pulsars detectable as point sources is

$$N_{\text{det}} \approx f \, N_{\text{tot}} \,.$$

For example, if $N_{\text{tot}} = 10^3$, then

$$N_{\text{det}} \approx 0.107 \times 10^3 \approx 107 \,.$$

Hence, one expects that on the order of 100 pulsars should be individually detectable as point sources by Fermi–LAT in the Galactic center region.

Conclusion

The framework outlined above provides one way to explain the spectral and morphological properties of the Galactic Center Excess via an unresolved population of pulsars. Adopting an NFW spatial distribution for the pulsars mimics the centrally concentrated morphology observed in the excess, while the power-law luminosity function with index $\alpha \sim 1.5$ and the typical spectral shape [Eq. (34)] are in agreement with what is observed from Fermi–LAT pulsars. These choices yield a total integrated flux that can be tuned to reproduce the GCE by adjusting the normalization of the luminosity function and the total number of pulsars.

4 Compute the sensitivity of Fermi-LAT for detecting dark matter in dwarf galaxies

Dwarf galaxies are among the cleanest targets for DM searches, since the astrophysical backgrounds are expected to be very low (with very little dust and an older stellar population) and contain few stars in comparison to normal galaxies.

The gamma–ray energy flux (in erg/cm^2/s) from a dwarf galaxy can be estimated using the expression

$$\Phi = \frac{\langle \sigma v \rangle}{8\pi\, m_\chi^2}\, N_\gamma\, J\,. \tag{41}$$

Considering that the sensitivity of Fermi-LAT around the GeV is

$$\Phi_{\text{th}} = 2 \times 10^{-12}\, \text{erg/cm}^2/\text{s}\,.$$

Compute the minimum annihilation rate at which Fermi-LAT can be sensitive, assuming the following:

- Detailed modeling of dwarfs typically yields astrophysical factors (when integrated over the dwarf's solid angle) in the range $J \sim 10^{18}$–$10^{19}\, \text{GeV}^2/\text{cm}^5$. Here, adopt

$$J = 10^{19}\, \text{GeV}^2/\text{cm}^5\,.$$

- N_γ is the effective energy yield per annihilation (in erg). For the $b\bar{b}$ channel the gamma–ray spectrum typically peaks at a few GeV. As a rough estimate, if we assume an average energy per photon of $\sim 2\,\text{GeV}$ and about 20 photons per annihilation, then the total energy yield is

$$20 \times 2\,\text{GeV} = 40\,\text{GeV}\,.$$

  Converting to erg ($1\,\text{GeV} \approx 1.6 \times 10^{-3}\,\text{erg}$), we have

$$N_\gamma \approx 40 \times 1.6 \times 10^{-3} \approx 6.4 \times 10^{-2}\,\text{erg}\,.$$

- Take $m_\chi = 50\,\text{GeV}$, so that $m_\chi^2 = 2500\,\text{GeV}^2$)

————

Answer:
Plugging Eq. (41) into this requirement:

$$\frac{\langle \sigma v \rangle}{8\pi\, m_\chi^2}\, N_\gamma\, J \geq 2 \times 10^{-12}\, \text{erg/cm}^2/\text{s}\,.$$

Solving for $\langle \sigma v \rangle$,

$$\langle \sigma v \rangle \geq \frac{8\pi\, m_\chi^2\, (2 \times 10^{-12})}{N_\gamma\, J}\,.$$

Let us now substitute the numerical values:

- $8\pi \approx 25.13$,

- $m_\chi^2 = 2500\,\text{GeV}^2$,

- $J = 10^{19}\, \text{GeV}^2/\text{cm}^5$,

- $N_\gamma = 6.4 \times 10^{-2}\,\text{erg}$,

- $\Phi_{\text{th}} = 2 \times 10^{-12}\, \text{erg/cm}^2/\text{s}$.

The numerator is:
$$8\pi\, m_\chi^2\, \Phi_{\rm th} \approx 25.13 \times 2500 \times 2 \times 10^{-12}\,.$$

Calculate:
$$25.13 \times 2500 = 62,825, \quad \text{and} \quad 62,825 \times 2 \times 10^{-12} = 1.2565 \times 10^{-7}\,.$$

The denominator is:
$$N_\gamma\, J = 6.4 \times 10^{-2} \times 10^{19} = 6.4 \times 10^{17}\,.$$

Thus,
$$\langle \sigma v \rangle \geq \frac{1.2565 \times 10^{-7}}{6.4 \times 10^{17}}\, {\rm cm}^3/{\rm s} \approx 1.964 \times 10^{-25}\, {\rm cm}^3/{\rm s}\,.$$

Rounding, we find
$$\langle \sigma v \rangle_{\rm min} \sim 2 \times 10^{-25}\, {\rm cm}^3/{\rm s}\,.$$

For a 50 GeV dark matter particle annihilating into the $b\bar{b}$ channel.

Conclusion For a typical dwarf spheroidal galaxy in the Milky Way with a mass of $\sim 10^7\, M_\odot$, an NFW profile characterized by $r_s \sim 15\,{\rm pc}$ and a scale density of order $100\, M_\odot/{\rm pc}^3$, and an integrated astrophysical factor $J \sim 10^{19}\, {\rm GeV}^2/{\rm cm}^5$, dark matter annihilating into the $b\bar{b}$ channel (with $m_\chi = 50\,{\rm GeV}$ and an energy yield of $\sim 6.4 \times 10^{-2}$ erg per annihilation) produces a gamma–ray flux given by Eq. (41). Requiring that the energy flux exceeds 2×10^{-12} erg/cm^2/s leads to a minimum annihilation cross section of approximately
$$\langle \sigma v \rangle_{\rm min} \sim 2 \times 10^{-25}\, {\rm cm}^3/{\rm s}\,.$$

This exercise shows that, for these assumed parameters, only if $\langle \sigma v \rangle$ is larger than about $2 \times 10^{-25}\, {\rm cm}^3/{\rm s}$ would the dwarf's dark matter annihilation signal exceed the sensitivity threshold.

References

[A+11]   M. Ackermann et al. Constraining dark matter models from a combined analysis of milky way satellites with the fermi large area telescope. *Physical Review Letters*, 107(24), December 2011.

[A+15]   M. Aguilar et al. Precision measurement of the proton flux in primary cosmic rays from rigidity 1 gv to 1.8 tv with the alpha magnetic spectrometer on the international space station. *Phys. Rev. Lett.*, 114:171103, Apr 2015.

[B+09]   M. Boezio et al. PAMELA and indirect dark matter searches. *New J. Phys.*, 11:105023, 2009.

[CCD+22]   Francesca Calore, Marco Cirelli, Laurent DEROME, Yoann Genolini, David Maurin, Pierre Salati, and Pasquale Dario Serpico. Ams-02 antiprotons and dark matter: Trimmed hints and robust bounds. *SciPost Physics*, 12(5), May 2022.

[CCW15]   Francesca Calore, Ilias Cholis, and Christoph Weniger. Background model systematics for the fermi gev excess. *Journal of Cosmology and Astroparticle Physics*, 2015(03):038–038, March 2015.

[CFK+23]   Marco Cirelli, Nicolao Fornengo, Jordan Koechler, Elena Pinetti, and Brandon M. Roach. Putting all the x in one basket: Updated x-ray constraints on sub-gev dark matter. *Journal of Cosmology and Astroparticle Physics*, 2023(07):026, July 2023.

[CKK17]   Alessandro Cuoco, Michael Krämer, and Michael Korsmeier. Novel dark matter constraints from antiprotons in light of ams-02. *Physical Review Letters*, 118(19), May 2017.

[CLH19]   Ilias Cholis, Tim Linden, and Dan Hooper. A robust excess in the cosmic-ray antiproton spectrum: Implications for annihilating dark matter. *Physical Review D*, 99(10), May 2019.

[DK12]   L. A. Dal and M. Kachelrieß. Antideuterons from dark matter annihilations and hadronization model dependence. *Physical Review D*, 86(10), November 2012.

[DlTLKB24] Pedro De la Torre Luque, Jordan Koechler, and Shyam Balaji. Refining Galactic primordial black hole evaporation constraints. *Phys. Rev. D*, 110(12):123022, 2024.

[DlTLWL24a] Pedro De la Torre Luque, Martin Wolfgang Winkler, and Tim Linden. Antiproton bounds on dark matter annihilation from a combined analysis using the DRAGON2 code. *JCAP*, 05:104, 2024.

[DLTLWL24b] Pedro De La Torre Luque, Martin Wolfgang Winkler, and Tim Linden. Cosmic-ray propagation models elucidate the prospects for antinuclei detection. *JCAP*, 10:017, 2024.

[DM21]   Mattia Di Mauro. Characteristics of the galactic center excess measured with 11 years of fermi-lat data. *Physical Review D*, 103(6), March 2021.

[DMW21]   Mattia Di Mauro and Martin Wolfgang Winkler. Multimessenger constraints on the dark matter interpretation of the fermi-lat galactic center excess. *Physical Review D*, 103(12), June 2021.

[EMBA20]   Carmelo Evoli, Giovanni Morlino, Pasquale Blasi, and Roberto Aloisio. Ams-02 beryllium data and its implication for cosmic ray transport. *Physical Review D*, 101(2), January 2020.

[KDF18]   Michael Korsmeier, Fiorenza Donato, and Nicolao Fornengo. Prospects to verify a possible dark matter hint in cosmic antiprotons with antideuterons and antihelium. *Physical Review D*, 97(10), May 2018.

[LN24]   Dylan M. H. Leung and Kenny C. Y. Ng. Improving HAWC dark matter constraints with inverse-Compton emission. *Phys. Rev. D*, 110(10):103021, 2024.

[LV18]   Paolo Lipari and Silvia Vernetto. Diffuse galactic gamma-ray flux at very high energy. *Physical Review D*, 98(4), August 2018.

[MP24]   Pankaj Munbodh and Stefano Profumo. Astrophysical constraints from synchrotron emission on very massive decaying dark matter. *Physical Review D*, 110(4), August 2024.

[Win17]   Martin Wolfgang Winkler. Cosmic ray antiprotons at high energies. *Journal of Cosmology and Astroparticle Physics*, 2017(02):048–048, February 2017.